Supplementary Information for:

$Ti_3C_2T_x$ MXene Flakes for Optical Control of Neuronal Electrical Activity

Yingqiao Wang[1], Raghav Garg[1], Jane E. Hartung[3], Adam Goad[4], Dipna A. Patel[4], Flavia Vitale[5, 6], Michael S. Gold[3], Yury Gogotsi[4], Tzahi Cohen-Karni[1, 2, *]

[1] Department of Materials Science and Engineering, Carnegie Mellon University, Pittsburgh, Pennsylvania 15213, United States.

[2] Department of Biomedical Engineering, Carnegie Mellon University, Pittsburgh, Pennsylvania 15213, United States.

[3] Department of Neurobiology, University of Pittsburgh, Pittsburgh, Pennsylvania 15213, United States.

[4] A.J. Drexel Nanomaterials Institute and Department of Materials Science and Engineering, Drexel University, Philadelphia, Pennsylvania 19104, United States.

[5] Department of Neurology, Department of Bioengineering, Department of Physical Medicine & Rehabilitation, and Center for Neuroengineering and Therapeutics, University of Pennsylvania, Philadelphia, Pennsylvania 19104, United States.

[6] Center for Neurotrauma, Neurodegeneration, and Restoration, Corporal Michael J. Crescenz Veterans Affairs Medical Center, Philadelphia, Pennsylvania 19104, United States.

[*] *Corresponding author: Tzahi Cohen-Karni- tzahi@andrew.cmu.edu*

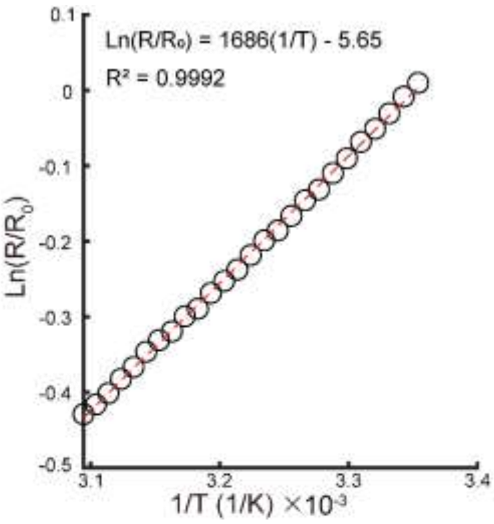

Figure S1. Micropipette calibration. A representative micropipette calibration curve. R_0 and R are the resistance of micropipette at room temperature and the resistance of micropipette at temperature T, respectively. Black circles denote the measured values and dashed red line denotes the linear fit.

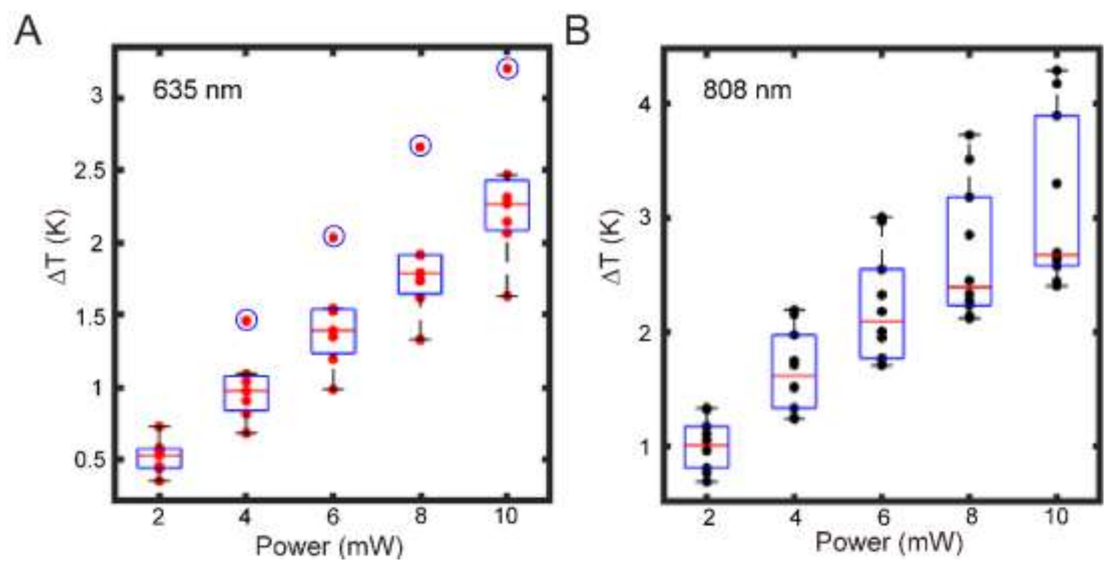

Figure S2. Photothermal response of isolated $Ti_3C_2T_x$ flakes under varying laser wavelengths. (A) Box plot of maximum temperature change measured for isolated $Ti_3C_2T_x$ flakes under 635 nm laser illumination with pulse width of 1 ms and varied powers (7 individual $Ti_3C_2T_x$ flakes were measured with 10 pulses per illumination condition). Solid red circles denote the temperature change at various powers. The central red line on each box indicates the median, and the bottom and top edges of the box indicate the 25th and 75th percentiles, respectively. Outliers are marked with blue circles. **(B)** Box plot of maximum temperature change measured for isolated $Ti_3C_2T_x$ flakes under 808 nm laser illumination with pulse width of 1 ms laser and varied powers (10 individual $Ti_3C_2T_x$ flakes were measured with 10 pulses per illumination condition). Solid black circles denote the temperature change at various powers. The central red line on each box indicates the median, and the bottom and top edges of the box indicate the 25th and 75th percentiles, respectively.

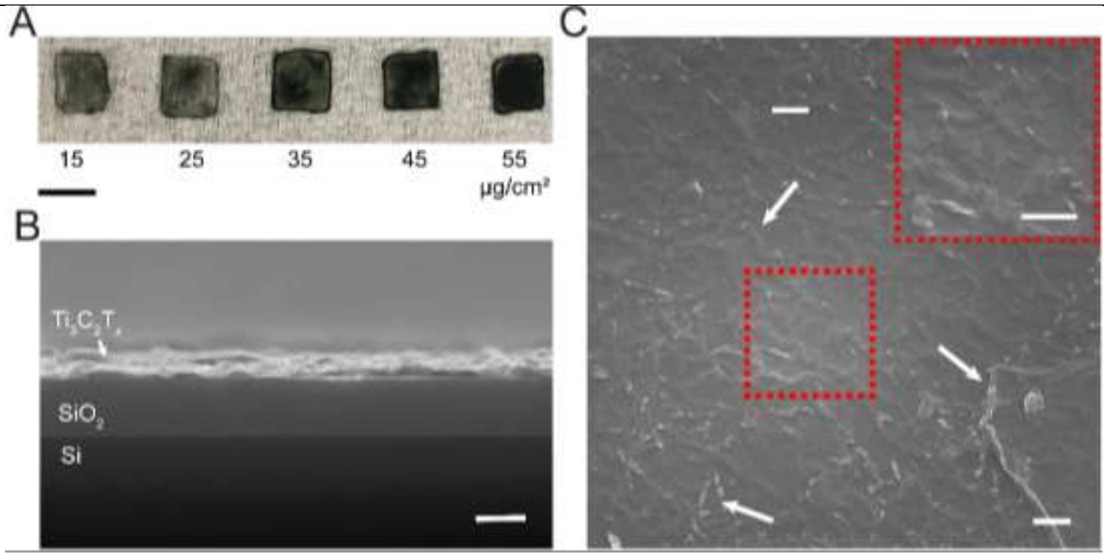

Figure S3. Characterization of $Ti_3C_2T_x$ films. (A) Optical image of different density $Ti_3C_2T_x$ films. Scale bar is 1 cm. **(B)** Cross section SEM of 25 μg/cm^2 $Ti_3C_2T_x$ film on Si/600 nm SiO_2 substrate. Scale bar is 500 nm. **(C)** Top view SEM of 25 μg/cm^2 $Ti_3C_2T_x$ film on glass substrate. White arrows denote wrinkles in the $Ti_3C_2T_x$ film. Inset is the expanded view of the dashed red box. Scale bars are 500 nm.

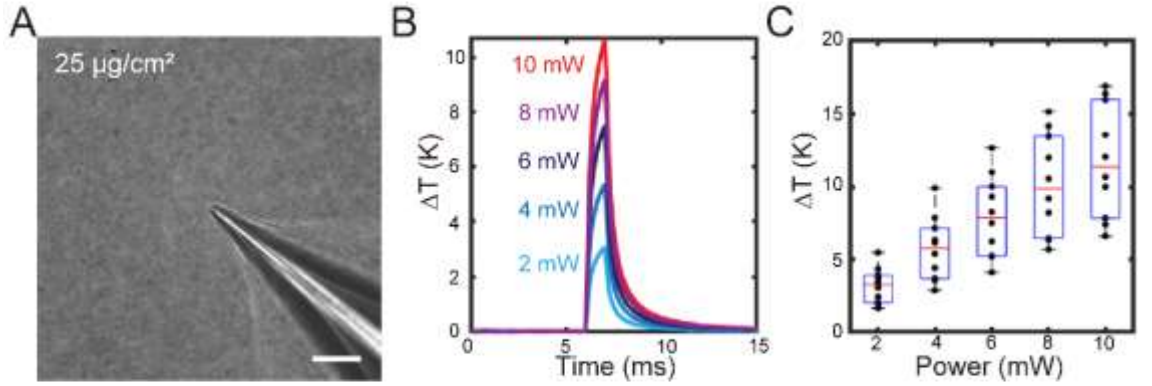

Figure S4. Photothermal response of $Ti_3C_2T_x$ films. (A) Optical image of 25 μg/cm^2 $Ti_3C_2T_x$ film with a glass micropipette. Scale bar is 20 μm. **(B)** Average temperature change as a function of time for a representative spot on 25 μg/cm^2 $Ti_3C_2T_x$ film under 635 nm laser illumination with pulse width of 1 ms and different incident laser powers. Presented data are the mean of 10 individual pulses. **(C)** Box plot of maximum temperature change measured for 25 μg/cm^2 $Ti_3C_2T_x$ films under 635 nm laser illumination with pulse width of 1 ms and varied applied power (10 individual spots were measured with 10 pulses per illumination condition). Solid black circles denote the temperature change at various powers. The central red line on each box indicates the median, and the bottom and top edges of the box indicate the 25th and 75th percentiles, respectively.

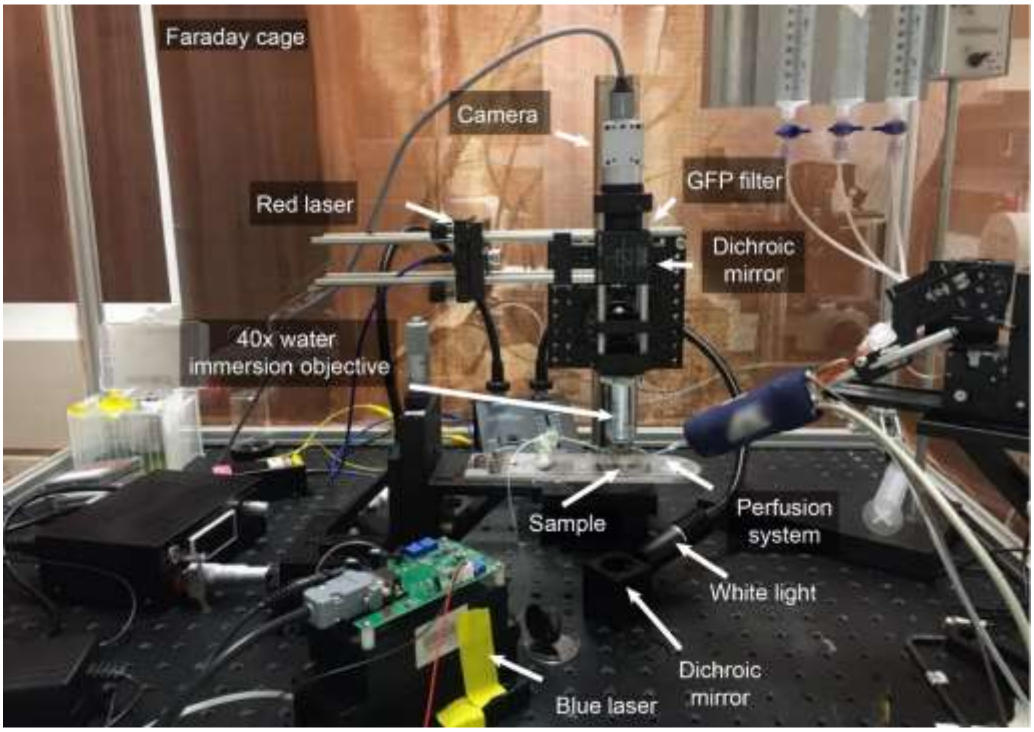

Figure S5. Photothermal stimulation microscope setup. Custom-built optical microscope for photothermal characterization of isolated $Ti_3C_2T_x$ flakes and Ca^{2+} imaging.

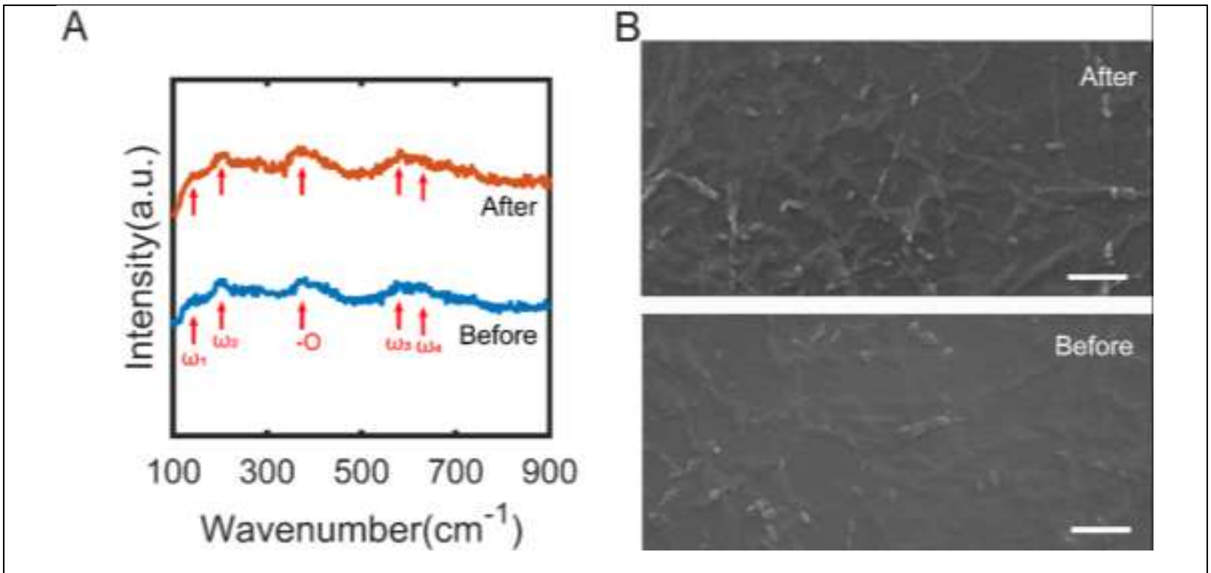

Figure S6. $Ti_3C_2T_x$ films have stable structure and composition in physiological condition for 7 days. (A) Raman spectra before and after incubating 25 µg/cm^2 $Ti_3C_2T_x$ films on glass coverslips (n = 3) at physiological condition (complete DRG media) in the incubator for 7 days. The red arrows indicate the characteristic peaks of $Ti_3C_2T_x$. **(B)** SEM images before and after incubating 25 µg/cm^2 $Ti_3C_2T_x$ films at physiological condition for 7 days. Scale bars are 500 nm.

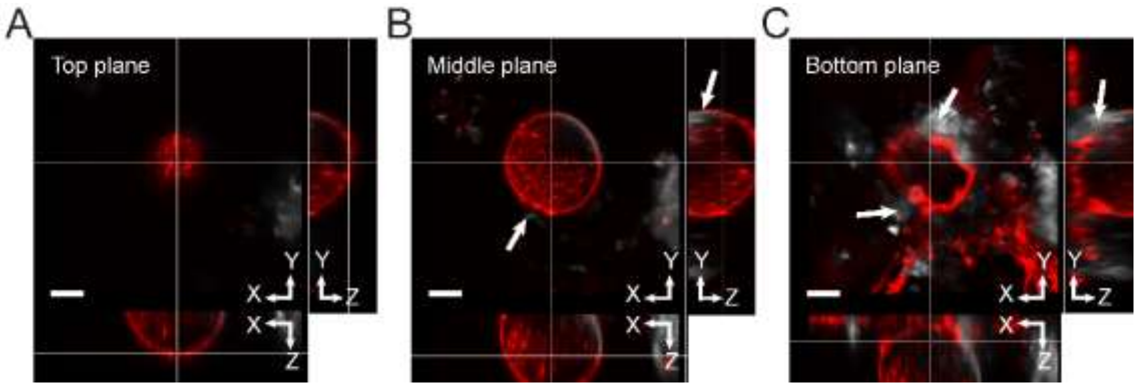

Figure S7. Orthogonal sections of DRG-$Ti_3C_2T_x$ flake interface at different Z-axis position. Orthogonal section images at the **(A)** top plane, **(B)** middle plane, and **(C)** bottom plane of a representative DRG neurons labeled with plasma membrane stain (red color, CellMask plasma membrane dye) incubated for 24 h with a dispersion of 100 µg/mL $Ti_3C_2T_x$ flakes (white color). The white arrows denote $Ti_3C_2T_x$ flakes. Scale bars are 10 µm.

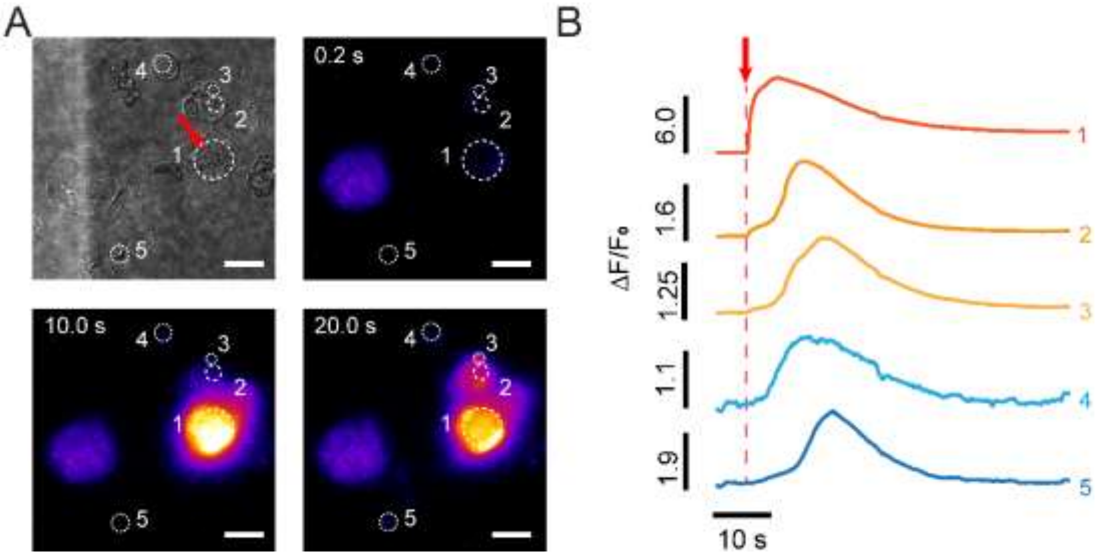

Figure S8. Modulation of 2D DRG network achieved by DRG-$Ti_3C_2T_x$ film interface is repetitive. (A) Bright field and time series fluorescence images of a representative DRG neuron interfaced with $Ti_3C_2T_x$ film and labeled with Ca^{2+} indicator (CalBryte 520 AM). A 635 nm laser pulse of 10 mW power and 1 ms pulse duration was applied at t = 5.4 s. Red arrow indicates the laser target spot. White circles denote the ROIs for fluorescence intensity analysis. Scale bars are 20 µm. **(B)** Normalized Ca^{2+} fluorescence intensity as a function of time for the cells marked in A. Red arrow denotes the starting point of the applied laser pulse (t = 5.4 s).

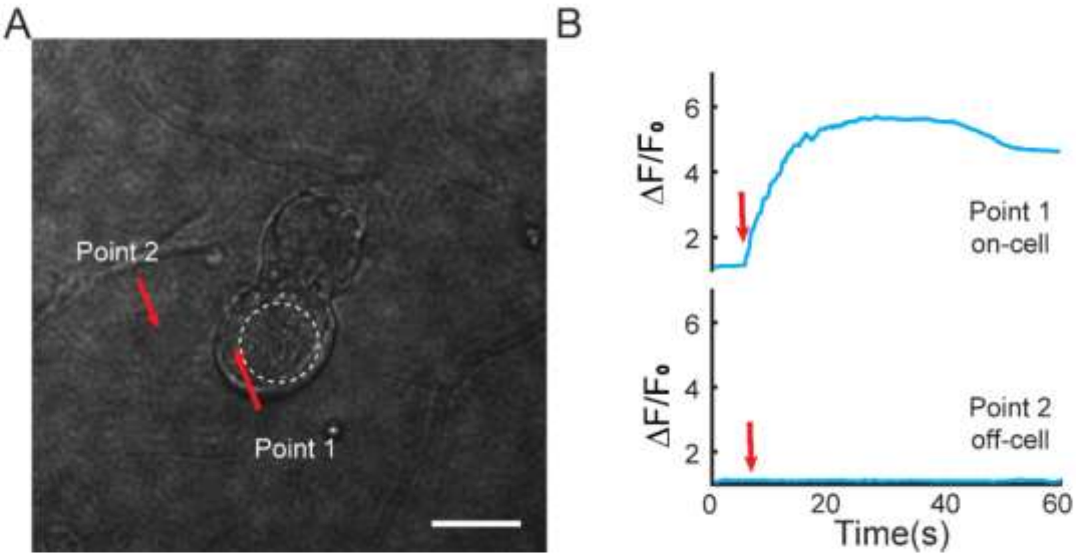

Figure S9. $Ti_3C_2T_x$ film enables selective modulation. (A) Bright field image of DRG neurons labeled with Ca^{2+} indicator dye (CalBryte 520 AM). 635 nm laser pulses of 2 mW power and 1 ms pulse duration were applied at t = 5.4 s (for both on-cell and off-cell illumination). White dashed circle denotes the targeted DRG neuron. Points 1 and 2 indicate the on-cell and off-cell illumination points, respectively. Scale bar is 20 µm. **(B)** Normalized Ca^{2+} fluorescence intensity as a function of time for the cell marked in A with on-cell and off-cell illumination. Red arrows denote the starting points of the applied laser pulse (t = 5.4 s for both on-cell and off-cell illumination).

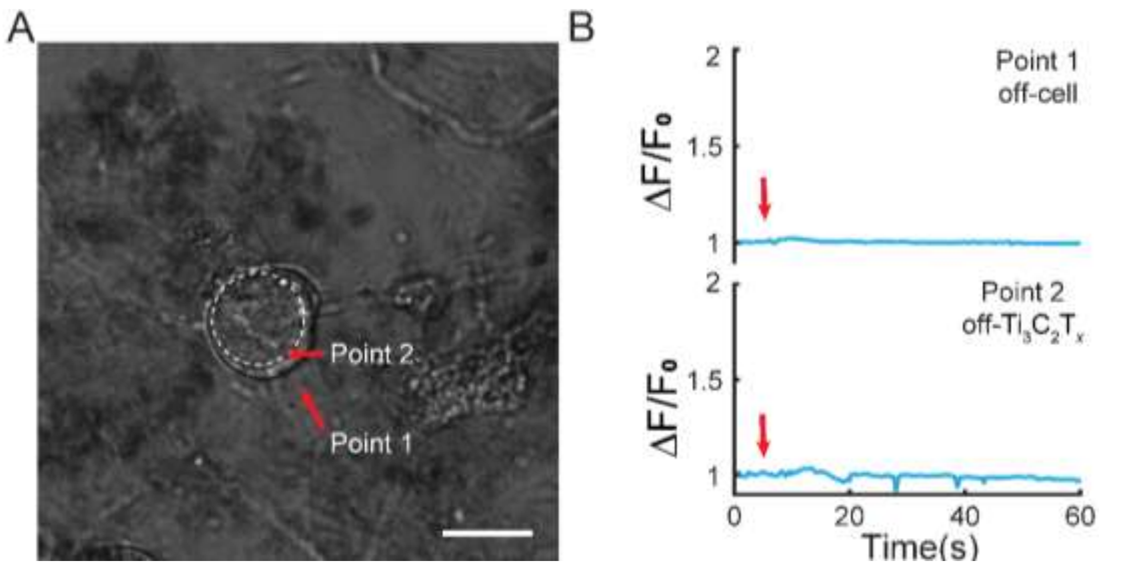

Figure S10. $Ti_3C_2T_x$ flakes enable higher selective modulation. (A) Control stimulation: off-cell and off-$Ti_3C_2T_x$ stimulation. Bright field image of DRG neurons labeled with Ca^{2+} indicator dye (CalBryte 520 AM). 635 nm laser pulses of 18 mW power and 1 ms pulse duration were applied at t = 5.0 s and 5.2 s for off-cell and off-$Ti_3C_2T_x$ illumination, respectively. White dashed circle denotes the targeted DRG neuron. Points 1 and 2 indicate the off-cell and off-$Ti_3C_2T_x$ illumination, respectively. Scale bar is 20 µm. **(B)** Normalized Ca^{2+} fluorescence intensity as a function of time for the cell marked in A with off-cell and off-$Ti_3C_2T_x$ illumination. Red arrow denotes the starting point of the applied laser pulse (t = 5.0 s and 5.2 s for off-cell and off-$Ti_3C_2T_x$ illumination, respectively).

Table S1. Data summary of AFM results of $Ti_3C_2T_x$ flakes.

Flake	**Average thickness (nm)**	**Standard deviation (nm)**
1	1.16	0.11
2	2.42	0.36
3	2.56	0.39
4	2.00	0.29
5	1.56	0.34
6	2.09	0.31
7	2.05	0.19
8	2.39	0.34
9	1.99	0.13
10	2.35	0.21
11	2.26	0.70
12	2.11	0.25
13	2.20	0.29
14	1.83	0.23
15	2.12	0.41
16	2.00	0.17
17	2.16	0.54
18	2.43	0.24
19	1.02	0.09
20	1.96	0.21
21	2.59	0.35
22	2.41	0.57
23	2.82	0.43
24	2.32	0.64
25	2.19	0.45
Average thickness	2.12	

Table S2. Data summary of the $Ti_3C_2T_x$ flakes' Raman spectra (n = 3, 10 spots per sample).

Sample	ω_1 (cm^{-1})	ω_2 (cm^{-1})	ω_3 (cm^{-1})	ω_4 (cm^{-1})
1	146.7	199.1	647.4	727.0
	147.4	199.0	634.7	721.9
	148.2	200.2	641.5	726.1
	148.8	200.9	636.0	722.0
	147.7	200.7	655.4	729.7
	149.2	200.0	633.2	718.3
	149.1	201.0	633.0	720.5
	148.1	200.2	634.2	721.2
	147.4	200.3	640.4	723.1
	149.7	201.1	635.5	720.2
2	149.0	199.9	636.2	731.1
	148.7	201.4	622.4	715.1
	148.2	199.0	605.2	723.3
	148.8	199.8	656.7	729.9
	145.4	200.3	637.1	716.6
	148.6	200.6	623.8	716.7
	149.2	200.2	675.5	755.4
	145.1	200.0	647.6	722.2
	146.8	198.6	650.5	720.7
	147.6	200.7	613.8	721.7
3	148.4	199.4	649.8	725.9
	146.8	201.7	639.3	733.6
	146.0	202.4	618.4	732.4
	145.2	201.6	669.6	727.6
	147.1	199.6	681.0	738.5
	142.2	203.2	586.7	727.1
	148.9	199.9	649.8	741.7
	147.3	199.1	638.3	728.3
	142.5	200.9	655.6	723.1
	146.4	201.3	636.0	720.7
Average	147.3	200.4	639.5	726.1
Standard Deviation	1.8	1.1	19.5	8.3

Table S3. Data summary of photothermal response measurement of isolated $Ti_3C_2T_x$ flakes (635 nm, 1 ms, 10 individual pulses per condition).

Flake	2 mW	4 mW	6 mW	8 mW	10 mW
1	0.44 ± 0.03	0.82 ± 0.02	1.20 ± 0.03	1.62 ± 0.02	2.06 ± 0.03
2	0.73 ± 0.02	1.46 ± 0.05	2.03 ± 0.03	2.66 ± 0.03	3.20 ± 0.02
3	0.36 ± 0.02	0.68 ± 0.02	0.99 ± 0.02	1.33 ± 0.03	1.63 ± 0.02
4	0.53 ± 0.02	0.98 ± 0.02	1.39 ± 0.01	1.79 ± 0.03	2.46 ± 0.02
5	0.56 ± 0.02	1.04 ± 0.02	1.53 ± 0.02	1.91 ± 0.03	2.31 ± 0.03
6	0.46 ± 0.04	0.91 ± 0.01	1.35 ± 0.02	1.74 ± 0.02	2.14 ± 0.02
7	0.58 ± 0.03	1.09 ± 0.04	1.54 ± 0.04	1.91 ± 0.03	2.26 ± 0.02

Table S4. Data summary of photothermal response measurement of isolated $Ti_3C_2T_x$ flakes (808 nm, 1 ms, 10 individual pulses per condition).

Flake	2 mW	4 mW	6 mW	8 mW	10 mW
1	0.68 ± 0.04	1.23 ± 0.04	1.76 ± 0.09	2.27 ± 0.03	2.62 ± 0.05
2	1.17 ± 0.02	1.97 ± 0.02	2.54 ± 0.02	3.18 ± 0.03	3.89 ± 0.04
3	0.80 ± 0.02	1.33 ± 0.01	1.76 ± 0.02	2.14 ± 0.02	2.40 ± 0.02
4	0.95 ± 0.02	1.51 ± 0.02	2.00 ± 0.01	2.33 ± 0.02	2.65 ± 0.02
5	1.04 ± 0.02	1.74 ± 0.01	2.32 ± 0.01	2.85 ± 0.02	3.30 ± 0.02
6	1.31 ± 0.02	2.19 ± 0.02	2.97 ± 0.03	3.72 ± 0.01	4.29 ± 0.02
7	0.76 ± 0.02	1.24 ± 0.01	1.70 ± 0.01	2.11 ± 0.02	2.44 ± 0.01
8	1.33 ± 0.03	2.15 ± 0.02	3.00 ± 0.01	3.51 ± 0.04	4.18 ± 0.02
9	1.10 ± 0.02	1.71 ± 0.02	2.17 ± 0.02	2.45 ± 0.01	2.69 ± 0.02
10	0.95 ± 0.02	1.51 ± 0.02	1.94 ± 0.02	2.23 ± 0.02	2.58 ± 0.01

Table S5. Data summary of photothermal response measurement of 25 μg/cm^2 $Ti_3C_2T_x$ films (635 nm, 1 ms, 10 individual pulses per condition).

Spot	2 mW	4 mW	6 mW	8 mW	10 mW
1	3.46 ± 0.04	6.15 ± 0.08	9.32 ± 0.09	11.98 ± 0.11	13.56 ± 0.19
2	3.94 ± 0.05	7.14 ± 0.08	10.00 ± 0.09	13.47 ± 0.11	15.98 ± 0.17
3	4.36 ± 0.07	7.86 ± 0.06	10.99 ± 0.08	14.16 ± 0.13	16.90 ± 0.28
4	5.48 ± 0.08	9.90 ± 0.06	12.67 ± 0.16	15.15 ± 0.07	16.39 ± 0.51
5	3.77 ± 0.02	6.35 ± 0.05	8.25 ± 0.04	10.56 ± 0.09	12.05 ± 0.13
6	1.97 ± 0.02	3.85 ± 0.04	5.19 ± 0.03	6.37 ± 0.04	7.84 ± 0.04
7	3.07 ± 0.03	5.38 ± 0.02	7.50 ± 0.04	9.19 ± 0.03	10.66 ± 0.05
8	1.65 ± 0.03	2.88 ± 0.04	4.11 ± 0.04	5.67 ± 0.05	6.60 ± 0.05
9	2.04 ± 0.03	3.69 ± 0.03	5.24 ± 0.02	6.45 ± 0.02	7.41 ± 0.04
10	2.43 ± 0.05	4.41 ± 0.02	6.23 ± 0.02	8.19 ± 0.04	9.99 ± 0.04

Table S6. Data summary of the illuminating laser condition (635 nm) on DRG-$Ti_3C_2T_x$ interfaces which induced the 2D DRG neuron network with various parameters.

Sample	Duration (ms)	Power (mW)	Energy (μJ)	Numbers of DRG Network
Film #1	1	10	10	1
Film #2	1	10	10	5
Film #3	1	10	10	1
	1	4	4	1
	1	2	2	2
Film #4	1	4	4	3
Dispersion #1	1	18	18	3

Table S7: Photothermal characterization of different agent using micropipette technique.

Nanomaterial Type	Nanomaterial Form	Light Wavelength (nm)	Spot Size (μm)	Incident Energy (J/cm^2)	Approx. Temperature Change (K)	Reference
Silica-coated Au nanorods (AuNRs)	Cluster	780	8.2	170	3.5	1
Au nanoparticles (AuNPs)	Cluster	532	~ 30	31	2	2
Intrinsic Si nanowires (i-SiNWs)	Individual	532	5	2398	5.4	3
Au-decorated SiNWs	Individual	532	5	240	2	4
Nanowire-Templated 3D Fuzzy Graphene (NT-3DFG)	Individual	635	20	3.18	6.0	5
$Ti_3C_2T_x$	Individual	635	20	3.18	2.3	This work
		808	20	3.18	3.3	This work
	Film	635	20	3.18	11.7	This work

Table S8. Summary of photothermal stimulation of DRG cells with various nanomaterials using 1 ms laser pulses.

Material Category	Material Form	Excitation Wavelength (nm)	Approx. Stimulation Energy Density for 1 ms Pulse	Reference
Au	Au nanoparticles (AuNPs)	532 nm	49.9 J/cm^2	6
	Functionalized AuNPs (AuNP-Ts1/SA/2abs)	532 nm	31 J/cm^2	2
	Au nanorods (AuNRs)	785 nm	26.4 J/cm^2	6
Si	Mesoporous Si particles	532 nm	6.8 J/cm^2	7
	Au-decorated SiNWs	592 nm	113 J/cm^2	4
C	Carbon nanotubes (CNTs)	405 nm	18.9 J/cm^2	6
		785 nm	85.7 J/cm^2	
	Graphite particles	405 nm	33.5 J/cm^2	6
	Nanowire-Templated 3D Fuzzy Graphene (NT-3DFG)	405 nm	0.9 J/cm^2	5
MXene	$Ti_3C_2T_x$ film	635 nm	0.6 J/cm^2	This work
	$Ti_3C_2T_x$ flakes	635 nm	5.7 J/cm^2	This work

Movie S1. Photothermal stimulation of a 2D DRG neuron network using $Ti_3C_2T_x$ film. Ca^{2+} imaging of a DRG network labeled with Ca^{2+} indicator dye (CalBryte 520 AM) seeded on a 25 µg/cm^2 $Ti_3C_2T_x$ film. A 635 nm laser pulse of 10 mW power and 1 ms pulse duration was applied at the DRG-$Ti_3C_2T_x$ interface at t = 5.6 s. The video was acquired at 5 frames per sec, processed in ImageJ, compressed to .mp4 format and sped up by 5×.

Movie S2. Photothermal stimulation of another 2D DRG neuron network using $Ti_3C_2T_x$ film. Ca^{2+} imaging of another DRG network labeled with Ca^{2+} indicator dye (CalBryte 520 AM) seeded on a 25 µg/cm^2 $Ti_3C_2T_x$ film. A 635 nm laser pulse of 10 mW power and 1 ms pulse duration was applied at the DRG-$Ti_3C_2T_x$ interface at t = 5.4 s. The video was acquired at 5 frames per sec, processed in ImageJ, compressed to .mp4 format and sped up by 5×.

Movie S3. Photothermal stimulation of a 2D DRG neuron network using $Ti_3C_2T_x$ flakes. Ca^{2+} imaging of a DRG network labeled with Ca^{2+} indicator dye (CalBryte 520 AM) incubated with 100 µg/mL $Ti_3C_2T_x$ flakes. A 635 nm laser pulse of 18 mW power and 1 ms pulse duration was applied at the DRG-$Ti_3C_2T_x$ interface at t = 5.0 s. The video was acquired at 5 frames per sec, processed in ImageJ, compressed to .mp4 format and sped up by 5×.

Reference:

1. Yong, J.; Needham, K.; Brown, W. G.; Nayagam, B. A.; McArthur, S. L.; Yu, A.; Stoddart, P. R., Gold-Nanorod-Assisted Near-Infrared Stimulation of Primary Auditory Neurons. *Advanced Healthcare Materials* **2014,** *3* (11), 1862-1868.
2. Carvalho-de-Souza, J. L.; Treger, J. S.; Dang, B.; Kent, S. B.; Pepperberg, D. R.; Bezanilla, F., Photosensitivity of Neurons Enabled by Cell-Targeted Gold Nanoparticles. *Neuron* **2015,** *86* (1), 207-217.
3. Jiang, Y.; Li, X.; Liu, B.; Yi, J.; Fang, Y.; Shi, F.; Gao, X.; Sudzilovsky, E.; Parameswaran, R.; Koehler, K., Rational Design of Silicon Structures for Optically Controlled Multiscale Biointerfaces. *Nature Biomedical Engineering* **2018,** *2* (7), 508-521.
4. Fang, Y.; Jiang, Y.; Acaron Ledesma, H.; Yi, J.; Gao, X.; Weiss, D. E.; Shi, F.; Tian, B., Texturing Silicon Nanowires for Highly Localized Optical Modulation of Cellular Dynamics. *Nano Letters* **2018,** *18* (7), 4487-4492.
5. Rastogi, S. K.; Garg, R.; Scopelliti, M. G.; Pinto, B. I.; Hartung, J. E.; Kim, S.; Murphey, C. G.; Johnson, N.; San Roman, D.; Bezanilla, F., Remote Nongenetic Optical Modulation of Neuronal Activity Using Fuzzy Graphene. *Proceedings of the National Academy of Sciences* **2020,** *117* (24), 13339-13349.
6. Carvalho-de-Souza, J. L.; Pinto, B. I.; Pepperberg, D. R.; Bezanilla, F., Optocapacitive Generation of Action Potentials By Microsecond Laser Pulses of Nanojoule Energy. *Biophysical Journal* **2018,** *114* (2), 283-288.
7. Jiang, Y.; Carvalho-de-Souza, J. L.; Wong, R. C.; Luo, Z.; Isheim, D.; Zuo, X.; Nicholls, A. W.; Jung, I. W.; Yue, J.; Liu, D.-J., Heterogeneous Silicon Mesostructures for Lipid-Supported Bioelectric Interfaces. *Nature Materials* **2016,** *15* (9), 1023-1030.